The crystal structure and phase transitions of the magnetic shape memory compound Ni_2MnGa

2002 J. Phys.: Condens. Matter 14 10159

(http://iopscience.iop.org/0953-8984/14/43/313)

INSTITUTE OF PHYSICS PUBLISHING JOURNAL OF PHYSICS: CONDENSED MATTER

J. Phys.: Condens. Matter **14** (2002) 10159–10171 PII: S0953-8984(02)38385-1

The crystal structure and phase transitions of the magnetic shape memory compound Ni_2MnGa

P J Brown[1,2], J Crangle[3], T Kanomata[4], M Matsumoto[5], K-U Neumann[1,6], B Ouladdiaf[2] and K R A Ziebeck[1,6]

[1] Physics Department, Loughborough University, Leicestershire LE11 3TU, UK
[2] Institut Laue-Langevin, BP 156, 38042 Grenoble Cedex 9, France
[3] Department of Physics, University of Sheffield, Sheffield S3 7RH, UK
[4] Faculty of Engineering, Tohuku Gakuin University, Tadajo 985-8537, Japan
[5] Institute of Multidisciplinary Research for Advanced Materials, Tohoku University, Sendai 980-8577, Japan

E-mail: K.R.Ziebeck@Lboro.ac.UK and K.U.Neumann@Lboro.ac.UK

Received 19 June 2002
Published 18 October 2002
Online at stacks.iop.org/JPhysCM/14/10159

Abstract

High resolution neutron powder diffraction and single crystal measurements on the ferromagnetic shape memory compound Ni_2MnGa have been carried out. They enabled the sequence of transformations which take place when the unstressed, stoichiometric compound is cooled from 400 to 20 K to be established. For the first time the crystallographic structure of each of the phases which occur has been determined. At 400 K the compound has the cubic $L2_1$ structure, and orders ferromagnetically at $T_C \approx 365$ K. On cooling below ∼260 K a super-structure, characterized by tripling of the repeat in one of the $\langle 110 \rangle_{\text{cubic}}$ directions, forms. This phase, known as the pre-martensitic phase, persists down to the structural phase transition at $T_M \approx 200$ K and can be described by an orthorhombic unit cell with lattice parameters $a_{\text{ortho}} = \frac{1}{\sqrt{2}} a_{\text{cubic}}$, $b_{\text{ortho}} = \frac{3}{\sqrt{2}} a_{\text{cubic}}$, $c_{\text{ortho}} = a_{\text{cubic}}$ and space group $Pnnm$. Below T_M the compound has a related orthorhombic super-cell with $b_{\text{ortho}} \approx \frac{7}{\sqrt{2}} a_{\text{cubic}}$, which can be described within the same space group. The new modulation appears abruptly at T_M and remains stable down to at least 20 K.

(Some figures in this article are in colour only in the electronic version)

1. Introduction

Ni_2MnGa is one of the group of 'shape memory effect' alloys which are currently exciting considerable interest. The origin of this effect in Ni_2MnGa is in the thermoelastic phase change

[6] Authors to whom any correspondence should be addressed.

which takes place at T_M on cooling through 200 K from the cubic $L2_1$ Heusler structure to a phase of lower symmetry [1]. If the material is plastically deformed in the low temperature martensitic phase and the external load removed it will regain its original shape when heated above the transition temperature. Based on early neutron diffraction data the transformation has been described as a simple contraction along one of the $\langle 100 \rangle$ directions of the cubic cell, without any change in the atomic positions. There is a strong deformation of the cell ($c/a \approx 0.94$) but only a 1% decrease in cell volume [2]. This phase transition is remarkable in that, in spite of the large deformation, it is reversible and a single crystal can be cycled through it many times without breaking. In recovering their shape the alloys can produce a displacement or a force, or a combination of the two, as a function of temperature. Because of these novel and remarkable properties shape memory alloys are helping to solve a wide variety of problems in both engineering and medicine [3]. Since Ni_2MnGa orders ferromagnetically below 365 K the possibility of producing giant field induced strains, which are an order of magnitude larger than those observed in rare-earth transition metal alloys, has stimulated a large number of investigations [4]. Despite the intense interest in Ni_2MnGa, the underlying physics and metallurgy are far from being understood. However, a precise knowledge of the transformation processes and the associated structures is fundamental in establishing the mechanisms involved, and it is with that objective that the current research was undertaken.

2. Previous work

2.1. Pre-martensitic behaviour

It has been suggested that the pre-martensitic phase occurs as a result of anharmonic coupling between the $[\zeta\,\zeta\,0]$ TA_2 phonon mode with homogeneous deformations associated with the Zener elastic constant $c' = (c_{11} - c_{12})/2$ [5]. The softening of the TA_2 phonon mode, observed in inelastic neutron scattering measurements [6], starts well above the transition temperature T_M. For a sample with $T_M = 220$ K the squared frequency of the mode with $\zeta = 0.325$ has a linear dependence on temperature $\nu^2 = a(T - T_\theta)$ as expected for soft mode behaviour. However, the intercept $T_\theta \approx 250$ K is significantly higher than T_M and the softening is incomplete with a reversal below 260 K. Thus in the region $T_\theta > T > T_M$ the $L2_1$ structure is predicted to be unstable to the formation of a pre-martensitic phase characterized by a 1/3, 1/3, 0 propagation vector. Ultrasonic measurements [7, 8] reveal that the magnitude of c', is anomalously low, namely 0.045×10^{11} N m^{-2} with a temperature variation which mirrors that of the soft mode frequency. Between 240 and 260 K c' decreases by ≈50% and on further cooling to T_M it increases by ≈30%.

2.2. Electronic structure

Electronic structure calculations for Ni_2MnGa show a peak in the density of states (DOS) at the Fermi level [9]. On the basis of these calculations it was argued that it is the redistribution of electrons around the Fermi level which drives the phase transition. The reduction in symmetry lifts the degeneracy of electron bands at the Fermi level, allowing the peak in the DOS to split. The reduction of free energy resulting from re-population of these bands may exceed that required to create the lattice distortion, in which case such a transformation is energetically favourable. A polarized neutron diffraction study of the magnetization distribution in Ni_2MnGa showed that the redistribution of unpaired spins in the phase transition is consistent with this *band Jahn–Teller* mechanism [10].

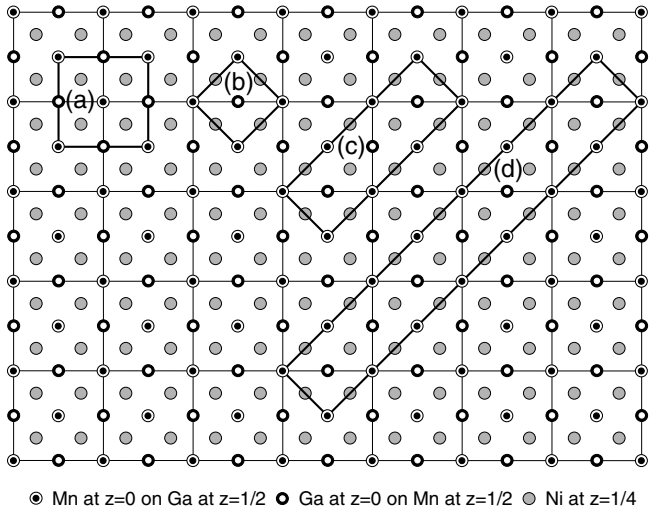

Figure 1. Projection on (001) of the ideal $L2_1$ Heusler alloy structure showing: (a) the $L2_1$ cell, (b) the body centred tetragonal unit cell, (c) and (d) the two orthorhombic super-cells. All the cells have the same c axis.

2.3. Structural investigations

On cooling, stoichiometric Ni_2MnGa undergoes a martensitic phase transition at $T_M = 200$ K. Early powder neutron diffraction measurements [2] report that above T_M the compound has the cubic Heusler $L2_1$ structure and below it a tetragonal modification with $a_t = 5.922$ and $c_t = 5.566$ Å. In addition to the tetragonal reflections some smaller peaks were observed and attributed to a modulation of the transformed lattice. An x-ray diffraction study of thermally and stress-induced martensites [11] showed similar super-structure reflections which indicated a 5-fold modulation of the (110) planes in the $[1\bar{1}0]$ direction of the bct martensite. A variant showing a 7-fold modulation was found in the stressed martensites. In addition to softening of the TA2 $[\zeta\,\zeta\,0]$ phonon neutron scattering measurements made on single crystals above T_M [6] showed a temperature-dependent peak in the elastic diffuse scattering with wavevector (1/3, 1/3, 0). Non-stoichiometric or stressed samples show different transformations and periodicities [12, 13]. The structure of the cubic phase and its relationship to the 3-fold and 7-fold modulated structures is shown in figure 1.

It is clear from all these investigations that the transformation process in Ni_2MnGa depends on the internal strain in the specimen. Many of the structural investigations have been carried out using electron diffraction and hence on very thin samples in which strains are likely to be present. Reports of recent diffraction experiments describe the transformed phase as being in a complex tetragonal state [14] and interpretation of these patterns has usually invoked the presence of more than a single phase. For most shape memory applications polycrystalline rather than single-crystal material will be used and it is important to establish the nature and structure of the phase transitions in polycrystalline Ni_2MnGa. We have therefore undertaken a detailed neutron powder diffraction investigation of a highly ordered stoichiometric sample of Ni_2MnGa supplemented by single-crystal intensity measurements of the precursor phase.

3. Experimental details

A 20 g sample of Ni_2MnGa was prepared by repeated melting of the constituent elements of 4 N purity in stoichiometric proportions in an argon arc furnace. The resultant ingot was

spark eroded to provide specimens suitable for specific heat, resistivity and magnetization measurements. The remainder of the ingot was crushed in a hardened steel pestle and mortar to a particle size of <250 μm. The powder and solid pieces were sealed under a reduced argon atmosphere in a quartz ampoule and annealed at 800 °C for 48 h, after which they were quenched in cold water. Subsequent x-ray powder diffraction measurements at room temperature confirmed that the sample was a single phase with the Heusler $L2_1$ structure (space group $Fm\bar{3}m$) and lattice parameter $a = 5.825$ Å. A single crystal of Ni_2MnGa was grown from the melt using the Bridgman technique; it was cylindrical in shape with length 30 mm and diameter 12 mm. A piece $\approx 3 \times 3 \times 8$ mm elongated parallel to $\langle 110 \rangle$, was cut from this sample for the single-crystal measurements.

The magnetization of the polycrystalline sample was measured in a field of 0.1 T using a SQUID magnetometer. An abrupt transition in the magnetization was observed at 200 K consistent with earlier measurements which identified the anomaly with the structural phase transition.

3.1. Neutron powder diffraction

The crystallographic structure of Ni_2MnGa was investigated as a function of temperature using neutron powder diffractometry. Powder diffraction patterns were obtained at five temperatures 400, 300, 220, 190 and 20 K, corresponding to the cubic, pre-martensitic and transformed phases, using the high resolution diffractometer D1A at the ILL Grenoble and a wavelength of 1.911 Å. The specimen was contained in a thin walled vanadium tube of diameter 7 mm mounted in an ILL cryo-furnace capable of providing temperatures stable to 0.2 K over the required range.

3.2. Single-crystal measurements

The single-crystal sample was mounted in the 4-circle cryostat of the diffractometer D10 at ILL Grenoble. The instrument was used in its 4-circle mode with a 32×32 pixel multidetector at a wavelength of 2.359 Å. At room temperature, the reflections observed were just those characteristic of the cubic Heusler alloy structure ($a = 5.822$ Å). On cooling to 190 K some small additional reflections appeared which could be indexed as $\boldsymbol{g} \pm \boldsymbol{\tau}$, where $\boldsymbol{g}$ is a reciprocal lattice vector of the fcc lattice and $\boldsymbol{\tau} = 1/3, 1/3, 0$. The evolution of the precursor phase was monitored by carrying out q scans along $hh0$ at 3 K temperature intervals between 300 and 200 K. Subsequently the integrated intensities of all the satellite peaks, generated using all members of the star of τ from all accessible reciprocal lattice vectors in the positive quadrant of reciprocal space, were measured at 230 and 215 K.

4. Results and data analysis

4.1. The cubic $L2_1$ phase 400–260 K

At 400 K Ni_2MnGa is in the paramagnetic state ($T_C = 365$ K). All eleven distinct Bragg peaks of the powder pattern (figure 2) observed in the angular range $2^\circ < 2\theta < 150^\circ$ could be indexed on a fcc lattice, giving further proof that the sample was a single phase. Profile refinement of the diffracted intensities confirmed that the specimen had the cubic $L2_1$ Heusler structure. Since the coherent nuclear scattering amplitudes of Ni, Mn and Ga are significantly different it was possible to determine the occupancies of the different sites. A statistical χ^2

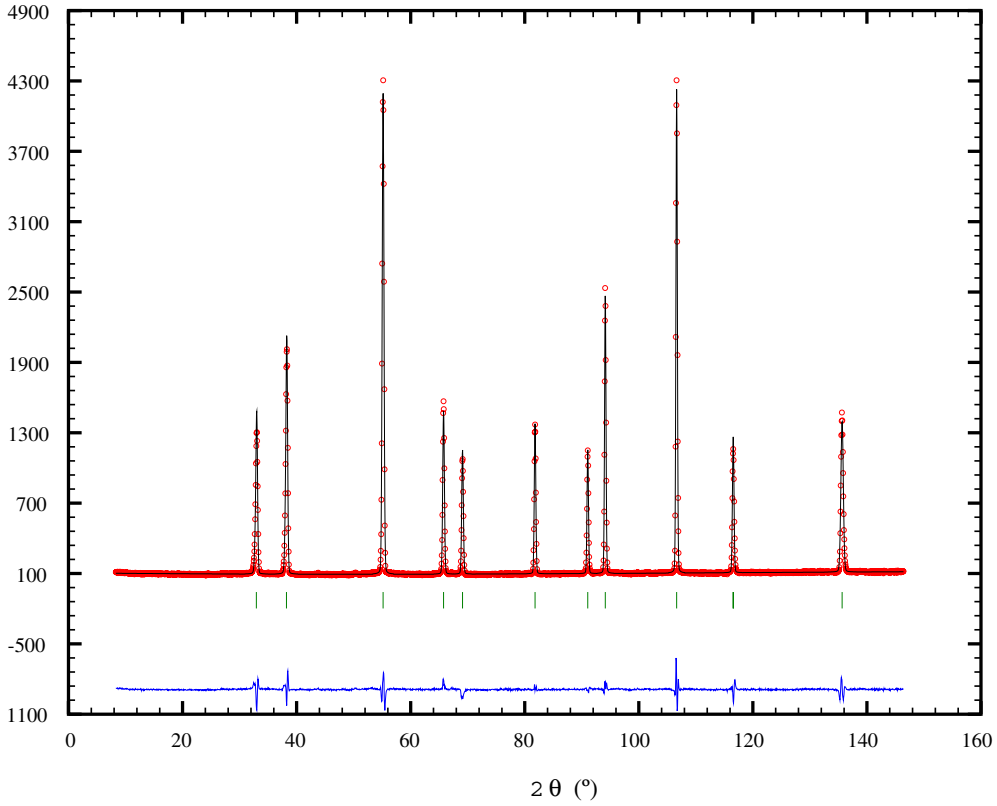

Figure 2. The observed and calculated neutron diffraction patterns of Ni_2MnGa in the paramagnetic phase at 400 K, together with the difference pattern.

test was applied to the fits obtained with the powder patterns; it is defined by

$$\chi^2 = \frac{(F_{obs} - F_{calc})^2/(\sigma F_{obs})^2}{N_{obs} - N_{par}} \tag{1}$$

where N_{obs} is the number of observations and N_{par} is the number of parameters. The results obtained in the refinement are given in table 1. They agree well with those reported earlier [2]. The observed and calculated diffraction patterns, together with the difference pattern, are shown in figure 2.

On cooling to 300 K there was no change in the number of Bragg reflections but there was an increase in intensity of those at low angle, consistent with the material becoming ferromagnetic. The profile refinement was carried out including a ferromagnetic moment on manganese with a Mn^{2+} form factor. The results are included in table 1 and the fitted pattern in figure 3. This shows that the structure does not distort on entering the ferromagnetic phase. The moment per Mn atom (2.4 μ_B) is in excellent agreement with the value obtained from magnetization measurements. A subsequent refinement was carried out in which the Ni atoms were also allowed to carry a moment but this did not improve the goodness of fit as indicated by the χ^2 test.

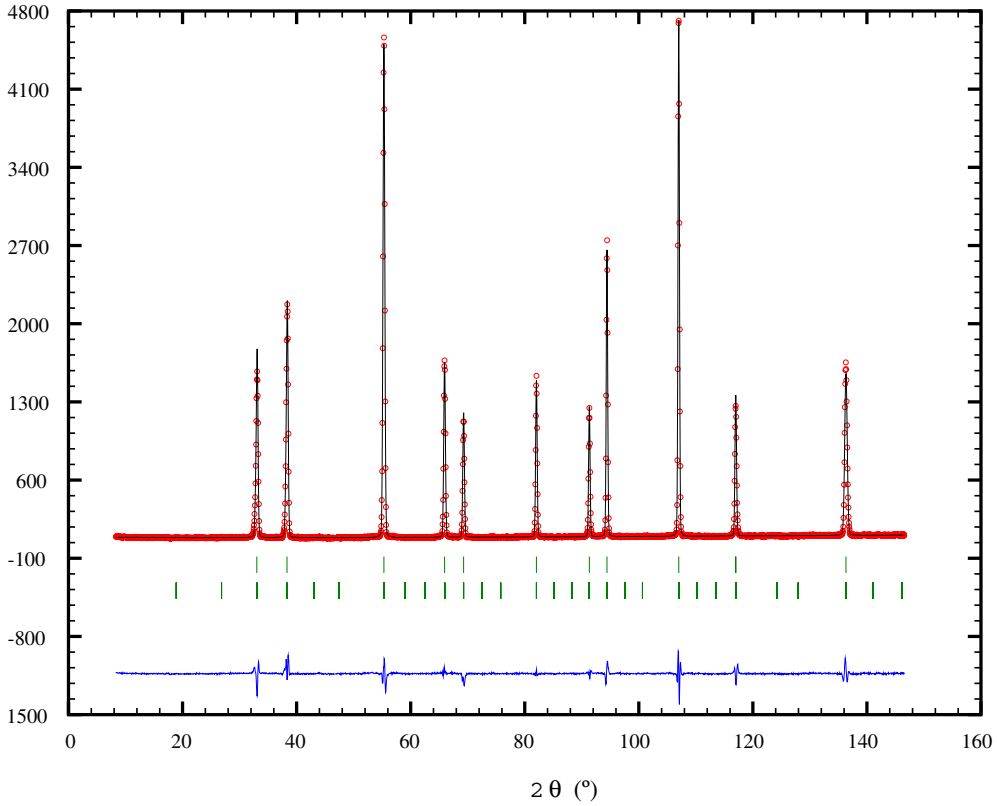

Figure 3. The observed and calculated neutron diffraction patterns of Ni_2MnGa in the ferromagnetic phase at 300 K, together with the difference pattern.

Table 1. Parameters of the cubic $L2_1$ structure of Ni_2MnGa determined from the profile refinement of neutron powder patterns at 300 and 400 K

Cubic Heusler $L2_1$ structure, space group $Fm\bar{3}m$		
Mn 4a 000	Ga 4b $\frac{1}{2}\frac{1}{2}\frac{1}{2}$	Ni 8c $\frac{1}{4}\frac{1}{4}\frac{1}{4}$
	300 K	400 K
a (Å)	5.8229(2)[a]	5.8636(2)[a]
	Ferromagnetic	Paramagnetic
Mn moment	2.4(2) μ_B	—
Mn occupancy	1	1
Ga occupancy	1	1
Ni occupancy	1	1
χ^2	4.9	4.7

[a] Relative to a neutron wavelength taken as 1.9110 Å.

4.2. The precursor phase: 255–200 K

The powder pattern obtained at 220 K is shown in figure 4. The main fcc peaks remain essentially unchanged but in addition a number of smaller peaks can be seen. The position of the smaller peaks could be accounted for using the 3-fold modulation of the lattice observed in the single-crystal data. The orthorhombic super-cell described below accounts for all the observed reflections.

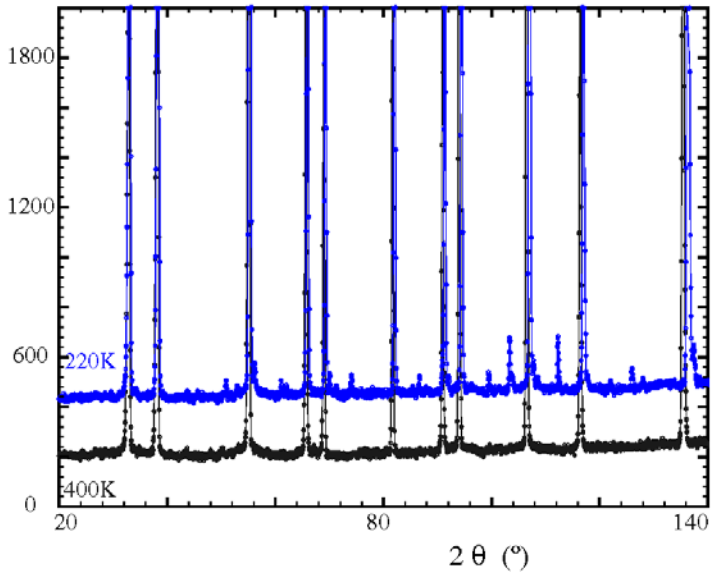

Figure 4. The observed neutron diffraction patterns of Ni_2MnGa in the pre-martensitic phase at 220 K (upper curve, shifted upwards), together with the pattern at 400 K (lower curve). The weak additional peaks in the 220 K pattern are indexed using a propagation vector of $\frac{1}{3}, \frac{1}{3}, 0$.

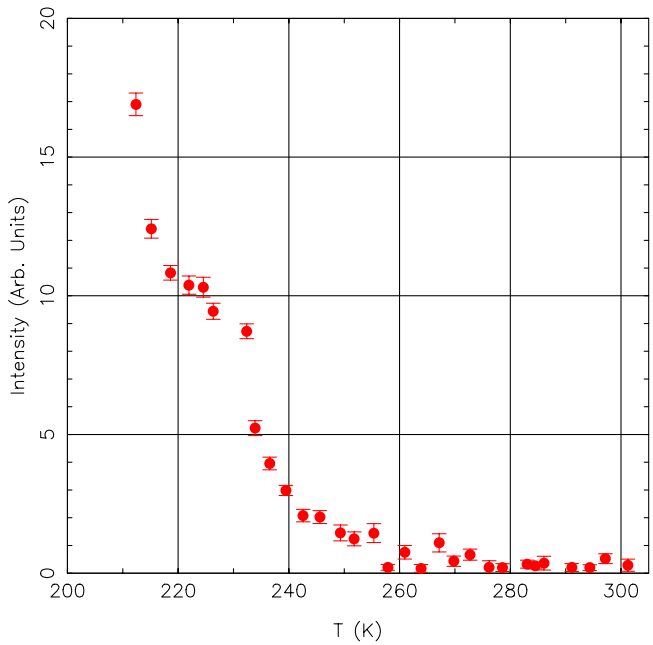

Figure 5. Temperature dependence of the mean integrated intensity of the $2\bar{2}0 \pm \tau$ reflections.

The evolution with temperature of the super-structure reflections belonging to the precursor phase in the single crystal is shown in figure 5. On cooling from 300 K the satellite reflections first became apparent around 255 K and increased continuously in intensity until, at ≈210 K, peak splitting associated with the cubic to orthorhombic transition intervenes. The q scan

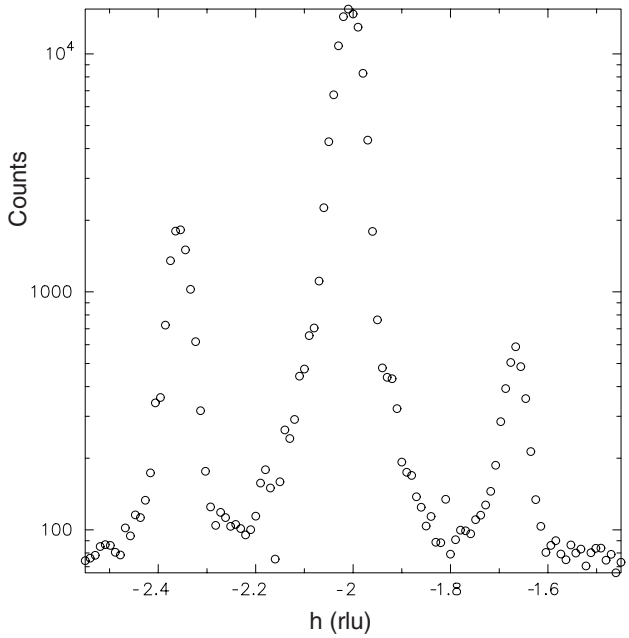

Figure 6. q scan along $h\bar{h}0$ through the $\bar{2}\bar{2}0$ reflection at 215 K.

recorded at 215 K is shown in figure 6. The fundamental and super-structure reflections in the precursor phase can be indexed on an orthorhombic unit cell with $a_{\text{ortho}} = \frac{1}{\sqrt{2}}a_{\text{cubic}}$, $b_{\text{ortho}} = \frac{3}{\sqrt{2}}a_{\text{cubic}}$ and $c_{\text{ortho}} = a_{\text{cubic}}$. There are six different domains, for one of which $a_{\text{ortho}} \parallel [110]_{\text{cubic}}$, $b_{\text{ortho}} \parallel [1\bar{1}0]_{\text{cubic}}$ and $c_{\text{ortho}} \parallel [001]_{\text{cubic}}$. The six domains which give the six-armed star of τ correspond to three different possible orientations of c_{ortho} ($[001]_{\text{cubic}}$, $[010]_{\text{cubic}}$ or $[100]_{\text{cubic}}$), for each of which a_{ortho} can have two different orientations.

For the integrated intensity measurements each reflection was assigned to its proper domain, and the domain populations estimated from reflections measured in more than one domain. The populations were used to scale and average all the measurements to obtain a set of integrated intensities for the super-structure reflections scaled to the whole crystal volume. These intensities were placed on an absolute scale by comparison with those of the fundamental reflections. The latter suffer severely from extinction at this wavelength, but the magnitude of the intensity reduction was estimated from measurements of the same crystal made at a shorter wavelength (0.84 Å) using the ILL instrument D9. The structure factors (F_{obs}) deduced in this way for the satellite reflections at 230 and 215 K are listed in table 2.

The intensities of the satellite reflections could be accounted for by a structure, similar to that proposed by [11] for martensites in stressed Ni_2MnGa crystals. In this structure the atoms in successive $(110)_{\text{cubic}}$ planes are displaced with respect to one another in the $[1\bar{1}0]_{\text{cubic}}$ direction by an amount which is modulated with a period of three lattice spacings in the $[110]_{\text{cubic}}$ direction. In the stressed crystals [11] the period was five lattice spacings. The modulated structure can be described in space group $Pnnm$ with the atomic positions given in table 3.

The variable x parameters of this structure were varied in a least squares refinement with respect to the structure factors measured for the satellite reflections. The refinement converged well giving the parameters reported in table 3. The structure factors calculated with these pa-

Table 2. Observed and calculated structure factors for satellite reflections of the precursor phase in units of fm per orthorhombic unit cell.

			230 K		215 K	
hkl			F_{obs}	F_{calc}	F_{obs}	F_{calc}
1	−2	0	1.96(12)	2.33	3.9(3)	4.85
1	1	1	1.26(8)	1.28	2.5(1.1)	2.57
0	−1	2	0.89(10)	0.00	1.9(2)	0.00
−1	−4	0	1.9(2)	2.33	4.4(3)	4.85
1	2	−2	5.13(4)	3.93	7.7(2)	6.78
2	−1	0	6.45(6)	7.85	13.41(5)	13.49
1	−5	1	0.9(9)	1.28	2.31(7)	2.57
1	−4	2	4.6(2)	3.93	7.3(2)	6.78
2	−2	1	1.50(7)	2.55	5.20(7)	5.11
1	1	−3	2.9(3)	1.28	1.9(2)	2.57
2	1	2	4.9(2)	4.66	9.67(4)	9.69
0	−4	3	0(2)	0.00	0.0(10)	0.00
2	4	1	3.94(10)	2.55	5.25(13)	5.11
2	−5	0	7.0(2)	7.85	14.1(6)	13.49
−1	−7	1	2.2(3)	1.28	2.4(2)	2.57
0	−7	2	0.0(7)	0.00	0.0(12)	0.00
0	−8	1	0.0(7)	0.00	1.2(1.2)	0.00
−1	−8	0	2.1(8)	2.33	3.4(3)	4.85
−1	−5	3	2.6(4)	1.28	2.4(3)	2.57
2	5	2	4.70(10)	4.66	9.5(3)	9.69
−2	−7	0	9.1(2)	7.85	16.1(8)	13.49
3	−2	0	7.12(7)	7.00	14.8(2)	14.52
1	2	−4	2.31(7)	2.33	4.9(2)	4.85
3	−1	1	6.2(3)	3.81	7.9(3)	7.58
1	−8	2	3.49(7)	3.93	6.1(7)	6.78
2	4	3	3.3(4)	2.55	5.35(10)	5.11
−1	−4	4	2.36(10)	2.33	4.4(2)	4.85
3	−4	0	6.96(10)	7.00	14.63(9)	14.52

rameters are listed in table 2. These calculations were made without taking the ferromagnetism into account. In a subsequent refinement a ferromagnetically aligned moment of 2.3 μ_B, the value obtained in the polarized neutron study [10], was associated with the Mn atoms. This refinement gave a significantly worse fit ($\chi^2 = 14$), suggesting that there may be a negative correlation between the Mn moment and its displacement. It should be pointed out that some significant intensity was measured in a few super-structure reflections with $h = 0$. These would be identically zero if the structural displacements were exactly in the cubic [110] direction.

The profile refinement of the powder pattern at 220 K was entirely consistent with this structure. However, the powder data do not define the displacement parameters well because the super-structure peaks are extremely weak and therefore the positional parameters given in table 3 are those obtained from the single-crystal data, whilst the manganese moment is that obtained in the powder refinement.

4.3. The martensitic phase: 200–20 K

Below 200 K the powder diffraction pattern is considerably more complicated. That obtained at 20 K is shown in figure 7. Some of the original fcc peaks split, the super-structure peaks observed at 220 K disappear and new peaks emerge. The number and position of the Bragg

Table 3. Structure parameters for the modulated phases refined in space group $Pnnm$. Only the values given as decimal fractions were refined.

			230 K[a]			215 K[a]			20 K[b]		
Atom position			x	y	z	x	y	z	x	y	z
2 Mn1	2a	000									
4 Mn2			0.013(2)	1/3	0	0.0218(5)	1/3	0	0.041(4)	1/7	0
4 Mn3	4g	$xy0$							−0.070(6)	2/7	0
4 Mn4									0.072(5)	3/7	0
2 Ga1	2b	$00\frac{1}{2}$									
4 Ga2			0.0015(9)	1/3	1/2	0.0051(2)	1/3	1/2	0.009(2)	1/7	1/2
4 Ga3	4g	$xy0$							0.026(2)	2/7	1/2
4 Ga4									0.062(1)	3/7	1/2
4 Ni1	4f	$\frac{1}{2}0z$			1/4			1/4			1/4
8 Ni2			0.4930(3)	1/3	1/4	0.4870(1)	1/3	1/4	0.476(1)	1/7	1/4
8 Ni3	8h	xyz							0.549(1)	2/7	1/4
8 Ni4									0.433(1)	3/7	1/4
Manganese moment (μ_B)					3.05(10)[c]				3.07(9)		
χ^2			10			9			9		

[a] Parameters refined from single-crystal data using only super-structure reflections and an orthorhombic unit cell with lattice parameters $a_{\text{ortho}} = \frac{1}{\sqrt{2}}a_{\text{cubic}}$, $b_{\text{ortho}} = \frac{3}{\sqrt{2}}a_{\text{cubic}}$, $c_{\text{ortho}} = a_{\text{cubic}}$.

[b] Parameters obtained from powder refinements using the whole pattern and a related orthorhombic unit cell with $b_{\text{ortho}} = \frac{7}{\sqrt{2}}a_{\text{cubic}}$.

[c] Magnetic moment from powder refinement at 220 K using the same unit cell as in [a].

peaks remains essentially the same between 200 and 20 K the lowest temperature at which measurements were made. The splitting of the Bragg peaks is consistent with the loss of cubic symmetry whilst the appearance of new peaks suggests that the translational symmetry is altered. An attempt to index the pattern using a tetragonal unit cell based on that reported by [2] was made. A cell with space group $I4/mma$ and lattice parameters $a = b = a_t/\sqrt{2} = 4.187$ Å and $c = c_t = 5.566$ Å could only account for some of the strong peaks. The possibility that the material had not fully transformed and that there remained a residual cubic component was also considered. However, the cubic unit cell did not account for the extraneous intense peaks. Closer inspection of the intense Bragg peaks, which above T_M were of the form $(h+k+l) = 2n$, suggested that they split into three at the transformation, indicating orthorhombic symmetry and the loss of the four-fold axis. Based on this observation a new analysis was carried out using the space group $Imma$. This space group could reproduce the splitting of the intense peaks but was unable to account for the additional weaker ones. Having established the nature of the transformation, the possible modifications to the orthorhombic cell which could account for the additional peaks were considered. A structure similar to that determined for the precursor phase but now with a 7-fold increase in the length of the b axis was able to account for all of the observed reflections. Using this new super-cell and space group $Pnnm$ a preliminary unit cell refinement was carried out. This analysis accounted for all of the observed peaks and did not generate any additional ones, confirming the correctness of the model. The refined lattice parameters are $a = 4.2152$, $b = 29.3016$ and $c = 5.5570$ Å. It may be seen that the degree of orthorhombic distortion $(a - b/7)$ is relatively small; it is only observable because of the high resolution of the diffractometer. A sequence of refinements based on this model was carried out in which the atomic positions were varied and the manganese atoms carried a ferromagnetic

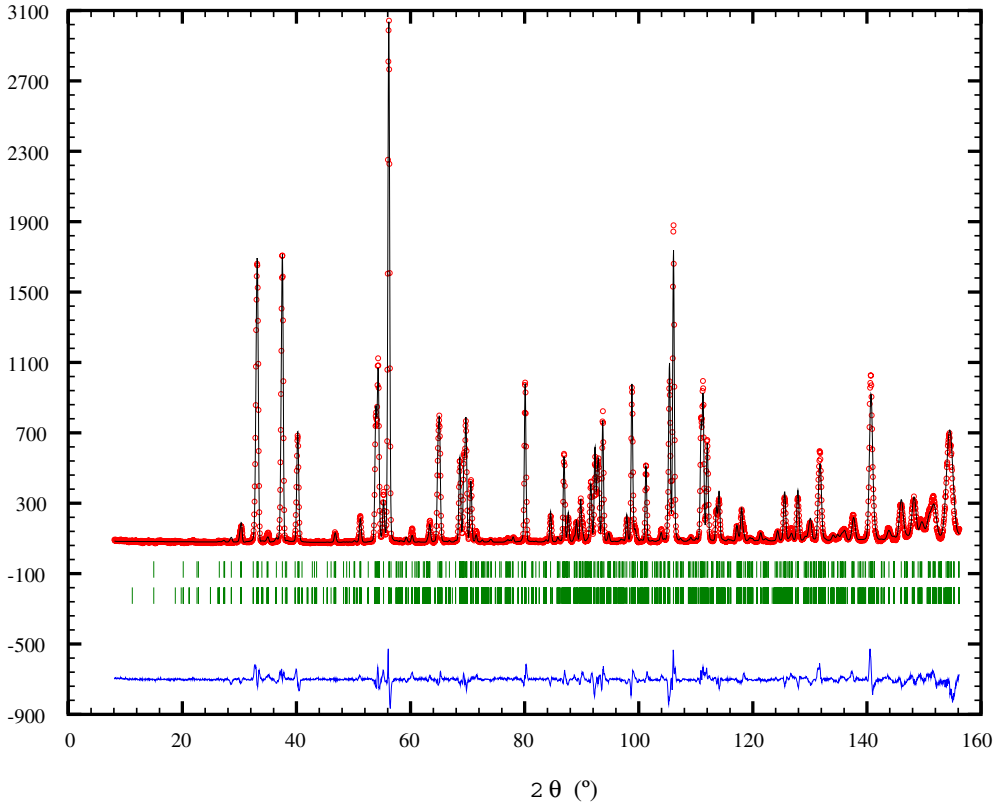

Figure 7. The observed and calculated neutron diffraction patterns of ferromagnetic Ni_2MnGa in the transformed phase at 20 K, together with the difference pattern.

moment. The results are given in table 3. As in the other refinements the moment was confined to the manganese atoms with the additional constraint that all four manganese atoms have the same moment. The moment was found to be oriented along the c axis. The diffraction pattern showing the quality of the agreement between the observed and calculated profiles is shown in figure 7.

5. Discussion

The results reported in the previous section have enabled the following sequence of structural phase transitions in the ferromagnetic shape memory compound Ni_2MnGa to be established.

Ferromagnetic		Ferromagnetic		Ferromagnetic		Paramagnetic	
Orthorhombic		Orthorhombic		Cubic		Cubic	
b=7a		b=3a		$L2_1$		$L2_1$	
4 K	$\longleftrightarrow$	200 K	$\longleftrightarrow$	260 K	$\longleftrightarrow$	360 K	$\longleftrightarrow$

The relationships between the unit cells of the three structurally different phases is illustrated in figure 1. The super-structures found for the two low temperature phases are derived from the cubic Heusler structure by a periodic displacement of the atoms in successive (110) planes along the $[1\bar{1}0]$ direction. This leads to an orthorhombic unit cell space group $Pnnm$ with $a_{\text{ortho}} \parallel [1\bar{1}0]_{\text{cubic}}$, $b_{\text{ortho}} \parallel [110]_{\text{cubic}}$, $c_{\text{ortho}} \parallel [001]_{\text{cubic}}$ and $a_{\text{ortho}} = \frac{1}{\sqrt{2}} a_{\text{cubic}}$, $b_{\text{ortho}} = \frac{n}{\sqrt{2}} a_{\text{cubic}}$,

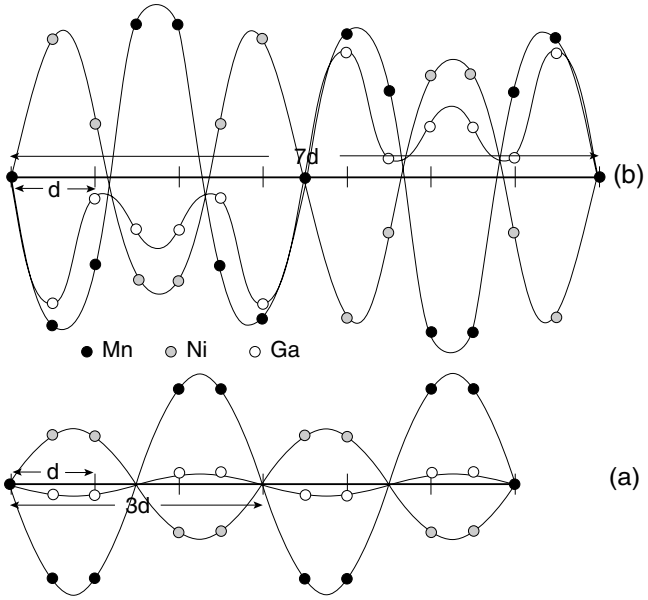

Figure 8. Displacements parallel to a_{ortho} of atoms in successive $(010)_{\text{ortho}}$ planes of (a) the pre-martensitic phase at 215 K and (b) the martensitic phase at 20 K. The displacements are represented on an arbitrary scale. For clarity that in (a) is twice that in (b). d is the lattice spacing of the cubic cell in the $\langle 110 \rangle$ direction $a_{\text{cubic}}/\sqrt{2}$.

$c_{\text{ortho}} = a_{\text{cubic}}$, where n is the periodicity of the displacement. The ability of neutrons to distinguish between manganese and nickel has allowed the individual atomic displacements to be determined for the first time. The displacement along a_{ortho} of the sublattices of Mn, Ni and Ga atoms in planes parallel to $(010)_{\text{ortho}}$ are plotted against their positions on the b_{ortho} axis in figure 8 for both the martensitic and pre-martensitic phases. It can be seen that, although the unit cells of the two phases are quite distinct, the modulation in the martensitic phase is far from sinusoidal and its dominant frequency is not very different from that of the pre-martensitic phase. In both structures the modulations of the Mn and Ni sublattices are out of phase and so the structural distortion is more nearly equivalent to a compression wave in the $(010)_{\text{ortho}}$ planes, propagating in the $[100]_{\text{ortho}}$ direction, than it is to a simple displacement of the planes. It should be pointed out that the structures refined for the martensitic and pre-martensitic phases are idealized ones in which the displacements have been constrained to the $[100]_{\text{ortho}}$ direction. There is some evidence in the intensities measured in the pre-martensitic phase for reflections with $h = 0$ that the structure may relax in other directions as well, but the present data are not sufficiently precise or numerous to determine the associated y or z displacements.

The change in the periodicity of the modulation from 3 to 7 at T_M appears to be an abrupt one without any intermediate steps. Once established at T_M the 7-fold modulation remains stable down to the lowest temperatures. Work in progress on a cold worked sample of Ni_2MnGa from the same ingot used in the present experiment shows that the 7-fold modulated structure remains stable down to 2 K. A 7-fold modulation has also been reported for shape memory alloys in the series Ni_xAl_{1-x} with $0.6 \leqslant x \leqslant 0.65$. In the symmetric phase the materials have the CsCl structure which is closely related to the Heusler structure through B2 disorder. On the basis of Landau analysis it has been proposed that the modulation arises again from an anharmonic coupling of a TA_2 phonon with the elastic constant c'. However, there is no

experimental evidence indicating a softening of a mode with $q = 1/7$ in Ni_2MnGa. The soft mode model has only been found to be appropriate for a very limited number of the known martensitic transitions [15]. The discovery of precursor effects above T_M has led to other models being proposed in which nucleation processes give rise to two length and time scales, one associated with atomic and the other with mesoscopic phenomena [16]. The atomic length scale has been addressed in the polarized neutron study [10] whereas the present paper focuses on the mesoscopic properties.

References

[1] Christian J W 1965 *Theory of Phase Transitions in Metals and Alloys* (London: Pergamon)
[2] Webster P J, Ziebeck K R A, Town S A and Peak M S 1984 *Phil. Mag.* **49** 295
[3] Gandhi M V and Thompson B S 1982 *Smart Materials and Structures* (London: Chapman and Hall)
[4] *Proceedings of SMART 2000*, Sendai, Japan
[5] Planes A, Mañosa L I and Vives E 1996 *Phys. Rev.* B **53** 3039
[6] Zheludev A, Shapiro S M, Wochner P, Schwartz A, Wall M and Tanner L E 1995 *Phys. Rev.* B **51** 11 310
[7] Stenger T E and Trivisonno J 1998 *Phys. Rev.* B **57** 2735
[8] Mañosa L, Gonzalez-Comas A, Obradó E, Planes A, Chernenko V A, Kokorin V V and Cesari E 1997 *Phys. Rev.* B **55** 11 068
[9] Fujii S, Ishida S and Asano S 1987 *J. Phys. Soc. Japan* **58** 3657
[10] Brown P J, Bargawi A Y, Crangle J, Neumann K-U and Ziebeck K R A 1999 *J. Phys.: Condens. Matter* **10** 4715
[11] Martynov V V and Kokorin V V 1992 *J. Physique* III **2** 739
[12] Vasil'ev A N, Bozhko A D, Khovailo V V, Dikshtein I E, Shavrov V G, Buchelnikov V D, Matsumoto M, Suzuki S, Takagi T and Tani J 1999 *Phys. Rev.* B **59** 1113
[13] Chernenko V A, Amengual A, Cesari E, Kokorin V V and Zasimchuk I K 1995 *J. Physique* C2 **5** 95
[14] Khovailo V V, Takagi T, Bozhko A D, Matsumoto M, Tari J and Shavrov V G 2001 *J. Phys.: Condens. Matter* **13** 9655
[15] Krumhansl J A and Goodings R J 1989 *Phys. Rev.* B **39** 3047
[16] de Gennes P G 1973 *Fluctuations. Instabilities and Phase Transitions* ed Riste (New York: Plenum)